JOURNAL OF MATERIALS SCIENCE 23 (1988) 1171–1181

Cyclic stress effects on the grain boundary cracking in Al–Mg solid solution

KYUNG TAE HONG, SOO WOO NAM
Department of Materials Science and Engineering, Korea Advanced Institute of Science and Technology, PO Box 131 Chongryang, Seoul, Korea

The difference in the grain boundary deformation between statically and cyclically crept specimens of Al–Mg solid solution has been investigated at the temperature of 580 K and for the peak stress level of 15 to 20 MPa. In statically crept specimens, the grain boundaries deform irregularly and no crack is formed either at the triple point or along the serrated boundaries. However, in cyclically crept specimens, where the stress frequency, stress amplitude and the ratio of on-load to off-load time are 3 cycles per minute, 90% of maximum peak stress and less than 1, respectively, the grain boundaries remain smooth and wedge-type cracks are formed at the triple points, which results in intercrystalline fracture. On the basis of the experimental observations it is believed that cyclic stressing enhances grain boundary sliding through an accelerated recovery with the help of mechanically generated excess vacancies during cycling. However, due to the constraints of the grain alignment, boundary sliding becomes very difficult and creates an intercrystalline fracture at a triple point. On the other hand, under static stress, since the grain boundary is serrated to decrease the stress concentration at a triple point, a crack hardly forms at the triple point.

1. Introduction

It is generally understood that, above the equicohesive temperature, the grain boundary region is weaker than the grain interior and creep rupture occurs in the intergranular fracture mode. For Al–Mg solid solution alloys near $0.45T_m$ at high stress, wedge-type cracks are formed mostly at the grain boundary triple points and this leads to intergranular creep rupture [1]. When grain boundary sliding appears to become a predominant process in static creep deformation, the amount of boundary sliding varies along the boundary [1] or in a periodic fashion [2], but near an obstacle such as a triple point, grain boundary sliding hardly occurs and this creates a stress accumulation at the obstacle. If this stress accumulation is not relaxed by recovery and/or plastic deformation near the obstacle, the stress accumulation becomes greater. Finally, the stress state can lead to the formation of a crack at this triple point and by this crack an intercrystalline fracture can be initiated [2, 3].

For cyclic creep, in which the stress alternates in a periodic fashion, the effects of the grain boundary on high-temperature cyclic creep deformation will be different from those on static creep, and the fraction of sliding in the total strain in cyclic creep will be different according to the stress mode, i.e. the stress frequency, amplitude and ratio of on-load time to off-load time.

For this work we have observed a very peculiar phenomenon of grain boundary cracking of Al–Mg solid-solution alloy due to cyclic stress. No grain boundary cracking occurs for static creep with the equivalent peak stress maintained constant. In this paper we investigate the effect of cyclic stressing on the grain boundary deformation and cracking.

2. Experimental procedures

The alloys for the specimens were fabricated by melting aluminium of 99.99% and magnesium of 99.9% purity. The chemical compositions of the specimens are tabulated at Table I. The slabs were homogenized for 72 h at 723 K and hot-forged at 673 K, then hot-rolled to a sheet of 3 mm thickness at 623 K and finally cold-rolled to a sheet of 1 mm thickness and machined along the rolling direction in the form of a plate-type tensile creep specimen to give the dimensions of gauge length and width as 25 and 4 mm, respectively. Prior to creep testing, most of the specimens were fully annealed at 773 K in a vacuum for 12 h to give an average grain size of about 0.3 mm, and air-cooled.

The creep tests were performed using a creep machine equipped with an Andrade–Chalmer constant-stress arm. The cyclic stress condition can be obtained with a specially designed cyclic loading machine [4] with which peak stress, stress amplitude and frequency can be controlled to have constant values during a test.

The extension of a specimen was measured by a Schaevitz Model HR 1000LVDT. The test temperature was 580 K and the peak stress level was not higher than 20 MPa. Two stress cyclic frequencies of 3 and 1 cycles per minute were applied, and the amplitudes of the cycling stress were 90% and 10% of the peak stress. A trapezoidal wave-shape of repeated tensile loading was used and for the calculation of the cyclic

0022–2461/88 $03.00 + .12

TABLE I Alloy compositions

Alloy	Composition (wt %)								
	Mg	Cu	Si	Fe	Zn	Ti	Cr	Sn	Al
Al–4% Mg	3.73	0.006	0.002	0.041	0.012	0.0009	0.0046	0.01	Balance
Al–2% Mg	1.49	0.020	0.000	0.039	0.012	0.0018	0.0064	0.02	Balance

creep rate, the total time for one cycle was used rather than the time of on-load only.

For optical metallographic studies, each specimen was carefully polished by mechanical and electrochemical methods [5] prior to testing, to give a mirror-like surface when examined by optical microscopy.

3. Experimental results

In the above-mentioned cyclic creep conditions, as is shown in Fig. 1, the apparent cyclic creep rate is smaller than that of static creep with the same peak stress by a factor of 0.9 (for Al–2% Mg). In this region, the stress exponent of static and cyclic creep is almost 3. The stress value used in this experiment (less than 20 MPa) is known to be smaller than the break-out stress of dislocations from the solute atmosphere [6]. So, in this stress region, it is believed that the creep deformation of the alloy is predominantly controlled by a dislocation glide process. Oikawa [7] has also reported a similar investigation for static creep by using an Al–Mg solid-solution alloy.

In cyclic creep, the specimens were ruptured with less than 50% of apparent creep strain but for the statically crept specimens no rupture was observed with more than 60% of true creep strain. For cyclic creep, before rupture, there were many grain boundary crackings which may contribute to the creep strain. It is observed experimentally that the rupture strain of cyclically crept specimen depends on the stress mode. Fig. 2 shows the cyclic creep curves of the different cyclic stress conditions. For the cyclic creep test with a stress frequency of 3 cycles per minute, stress amplitude of 90% and peak stress of 15 MPa, the rupture strain is observed to be about 40%; however, when a frequency of 1 cycle per minute is applied with other conditions unchanged, the specimen is not ruptured up to 60% of creep strain. However, for tests with a stress amplitude of 10% of the peak stress, regardless of the value of the peak stress (15 or 20 MPa), the specimens are not ruptured with a strain of up to 60%, which is the maximum strain we can get with our test machine.

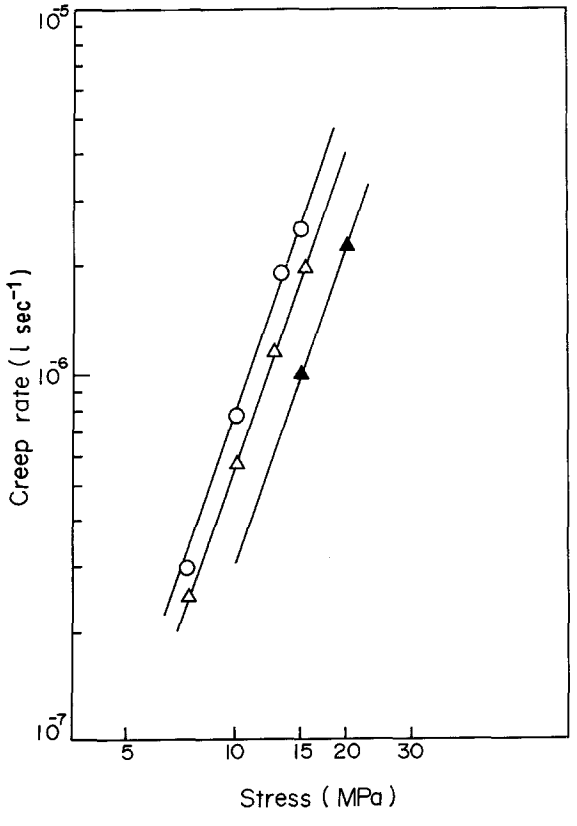

Figure 1 Cyclic and static creep rate against stress at 580 K. (○) Static, 2% Mg; (△) cyclic, 2% Mg; (▲) cyclic, 4% Mg.

It is of interest to see how the rupture strain varies with the ratio of t_u/t_l (t_u = off-load time, t_l = on-load time). Fig. 3 shows the effect of the ratio of off-load to on-load time, with the fixed test condition of 15 MPa, 3 cycles per minute and $\Delta\sigma/\sigma = 90\%$, on the rupture strain. With a value of $(t_u/t_l) = 9$, the specimen has ruptured with a strain of almost 3%, but as the value of t_u/t_l becomes smaller, the rupture strain increases. The fracture mode of a cyclically ruptured specimen is observed to be a typical intercrystalline fracture as shown in Fig. 4. The cracked surface is sharp and the crack is formed along the grain boundaries at the triple point, inclined 45° about the stress axis. In the same specimen, depending on the grain, we have also observed the rotation of a grain during cyclic creep deformation (Fig. 5).

From the static creep curves shown in Fig. 2 one can see the normal primary stage, but for the cyclic creep curve an inverted primary stage is observed with a peak stress of 15 MPa. By changing from the cyclic to the static stress mode at a steady state of cyclic creep deformation, we can see that the normal primary stage occurs after the mode change (Fig. 6). So it may be said that the internal structure of the specimen under cyclic loading is equivalent to that of the primary stage of the statically crept specimen.

The deformation behaviour of the grain boundary is experimentally observed to be affected by the stress mode. In the static stress mode with a peak stress of 15 MPa, the grain boundary is severely serrated as shown in Fig. 7, while under the cyclic mode the grain boundary is negligibly serrated (Fig. 8). However, as shown in Fig. 8a, there has been a significant amount of grain boundary sliding during cyclic creep. The grain boundary structure seems to affect the behaviour of the grain boundary sliding. In addition to the sliding, there is marked grain boundary deformation around the obstacle which hinders the grain boundary

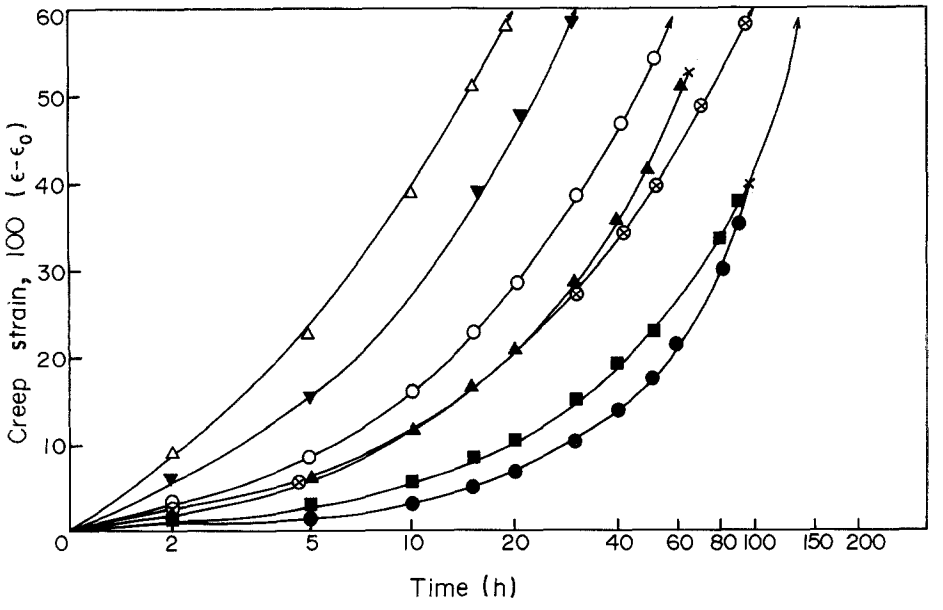

Figure 2 Cyclic and static creep curves at 580 K. Cyclic, 3 cycles per minute: (⊗) $\Delta\sigma/\sigma$ = 0.1, 15 MPa; (●) $\Delta\sigma/\sigma$ = 0.9, 15 MPa; (▼) $\Delta\sigma/\sigma$ = 0.1, 20 MPa; (▲) $\Delta\sigma/\sigma$ = 0.9, 20 MPa. Cyclic, 1 cycle per minute: (■) $\Delta\sigma/\sigma$ = 0.9. Static: (○) 15 MPa, (△) 20 MPa.

sliding (Fig. 8), and the formation of folds in the opposite grain (Fig. 9) or the rotation of the grain at the triple point (Fig. 5). For polycrystals, all of the above-mentioned phenomena can be observed independent of the stress mode in the cyclic creep but, for static creep, the rotation of grain boundaries is not observed. On the other hand, the grain boundary is relatively smooth in the cyclically crept specimen and there exists a crack or a rotation of the grain boundary at a triple point. Since the above-mentioned observations are confined to the surface of the specimen, to see the behaviour of the boundary inside the specimen, the surface of the crept specimen was carefully polished off and etched. As shown in Fig. 10, with a decreasing ratio of off-load to on-load time (t_u/t_l) the shape of the grains is changed from equiaxed to an elongated shape, or from a smooth grain boundary to an irregular one. Rachinger [8] measured the fraction of sliding to the total deformation by using a relation such as $\varepsilon_g = \bar{W}^{2/3} - 1$, where $\bar{W} = \bar{b}/\bar{a}$ and $\bar{b}$ is the length of the grain along the stress axis, $\bar{a}$ is the length of the grain perpendicular to the stress axis and ε_g is the average strain of the grain. By using this method in our experiments, we obtained the fraction of the sliding in the total deformation as a function of t_u/t_l, and the results are tabulated in Table II. In the annealed state before the creep experiment, the shape of the grain is equiaxed ($\bar{W}$ = 1.0214). As t_u/t_l decreases, the fraction of grain boundary sliding increases and the rupture strain decreases.

It is intended to investigate the effects of the loading rate on the amount of sliding and rupture strain as the loading rate (from unloaded state to loaded state for a half cycle) is decreased from 15 MPa in 0.3 sec to

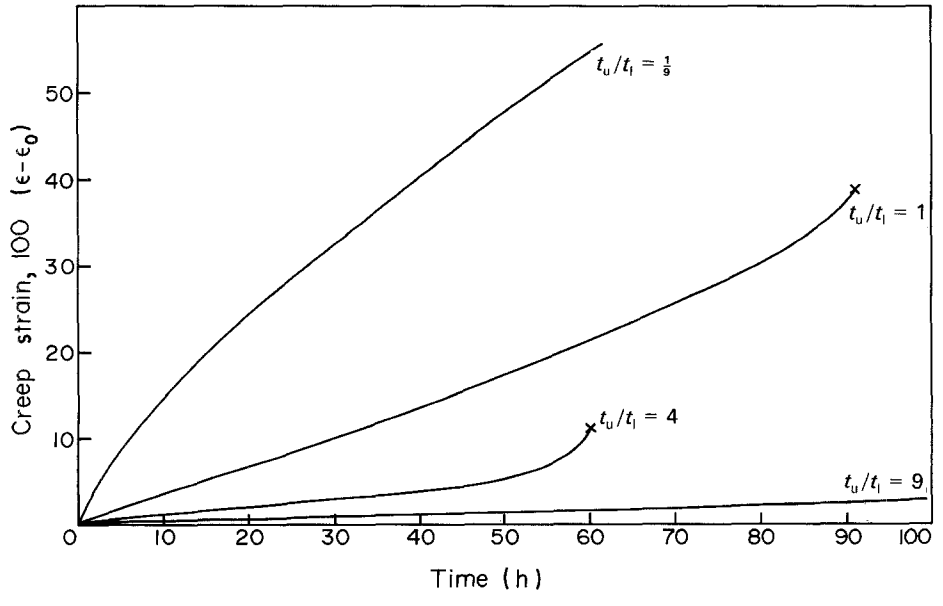

Figure 3 Cyclic creep curves for various ratios of on-load to off-load time at 580 K. Stress = 15 MPa, frequency = 3 cycles per minute, stress amplitude = 90%.

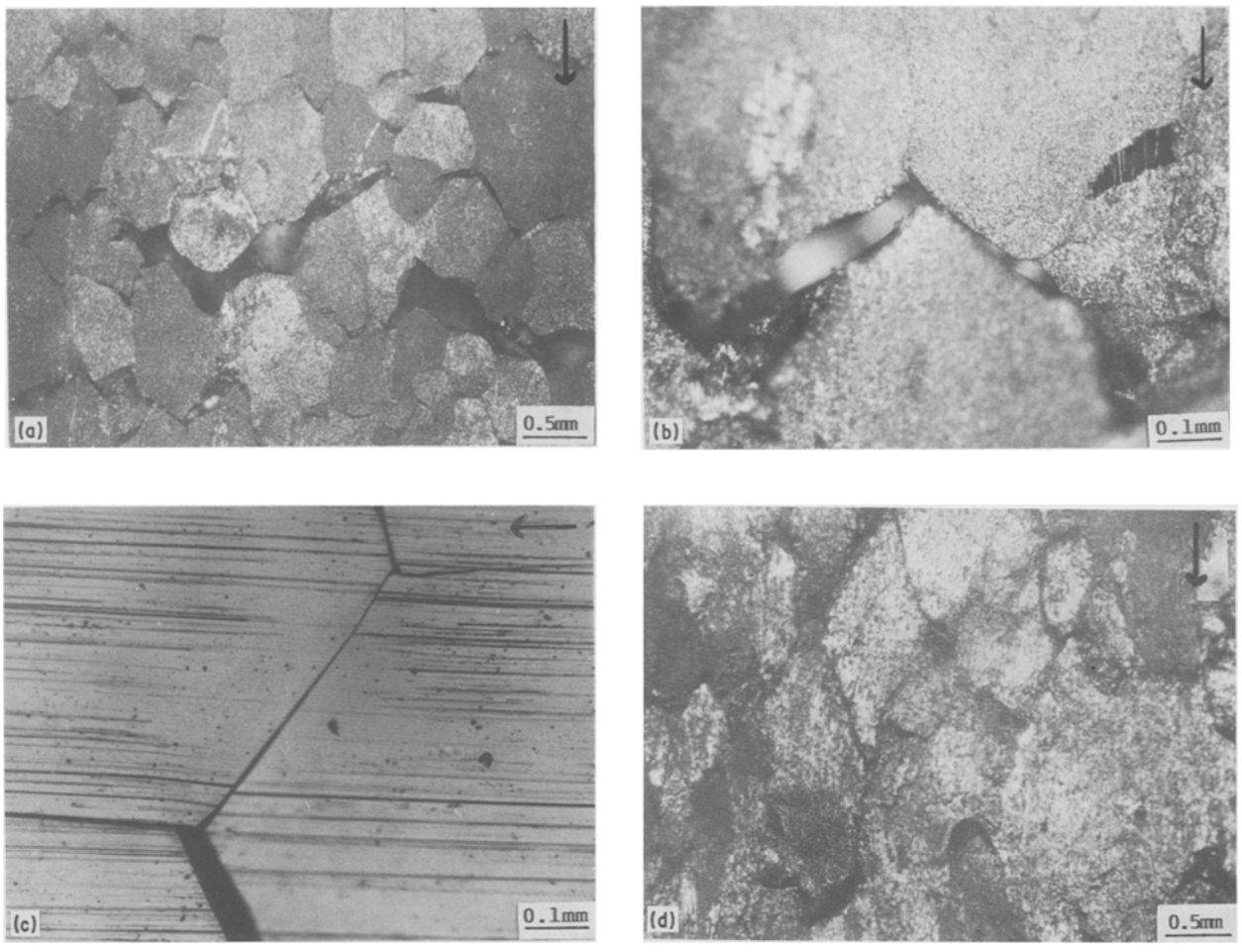

Figure 4 Metallographic observation of cyclically crept specimens. (a, b) Peak stress 15 MPa, stress frequency 3 cycles per minute, stress amplitude 90%; (c) cyclic creep after electropolishing and surface marking, same stress conditions as (a); (d) Statically crept specimen, stress 15 MPa. Arrows indicate the stress axis.

15 Mpa in 2.1 sec. In these experiments, the rupture strain in the slow loading rate is measured to be larger than that in the fast loading rate. The fraction of sliding in the total deformation is slightly decreased with the slow loading rate. Therefore, it is understood that the loading rate affects the grain boundary sliding and so the cracking at a triple point.

4. Discussion

4.1. Grain boundary deformation at the triple point

The stress accumulation by grain boundary sliding can occur at triple points during static creep as suggested by Grant and co-workers [1–3] or at ledges as Snowden [9] reported. If this accumulated stress is not

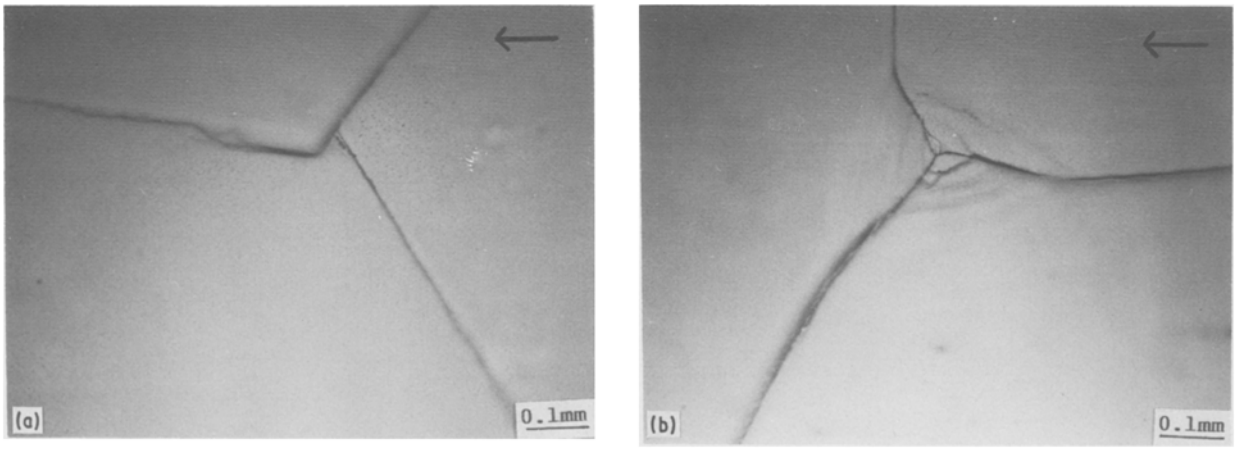

Figure 5 (a, b) Metallographic observation of cyclically crept specimens (triple point). Cyclic stress conditions 15 MPa, 3 cycles per minute; stress amplitude = 90%; amount of creep strain = 5%.

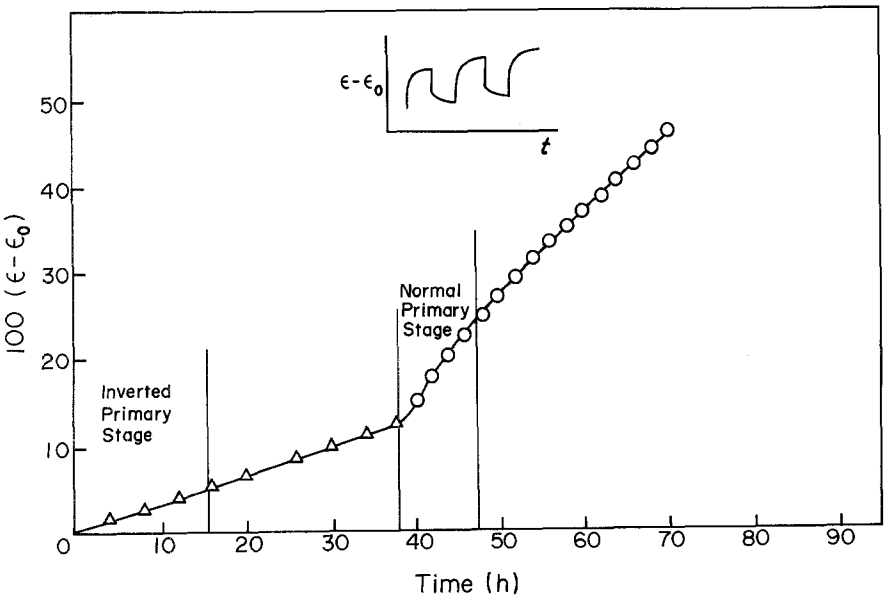

Figure 6 Mode change from (△) cyclic to (○) static creep at 580 K. Stress 15 MPa.

relaxed but increased to the level of the rupture stress, then a crack can be formed at these obstacles [9, 10]. To relax the accumulated stress, one of the following processes is observed to be responsible, i.e. the formation of a fold in one grain, severe deformation of grain corners at a triple point, or a rotation of grains (Fig. 5). Since, in the same specimen, all of the above-mentioned phenomena of stress relaxation at the triple points are observed, it may be hypothesized that the main relaxation process may vary for different grain boundaries with distinct characteristic properties. If a grain boundary is deformed irregularly, a ledge can be deformed to become the obstacle such that it may reduce the distance between the new stress-accumulating points (Fig. 7). Because the strength of concentrated stress at the obstacle is known to be proportional to the distance between the stress accumulating points as suggested by Stroh [10, 11], the stress accumulation is reduced at a triple point in an irregularly deformed grain boundary. This behaviour is clearly observed in statically crept Al–Mg specimens (Fig. 7) and in lead [9]. However, in a cyclically crept specimen with a smooth grain boundary, this tendency is reduced to a small extent so that a crack is formed along the grain boundary at a triple point by the large stress accumulation (Fig. 10).

4.2. Cyclic stress effects on the stress exponent

In spite of the difference in rupture mode, rupture strain and grain boundary deformation behaviour (Fig. 4, Table II), it is experimentally verified that the stress exponents of the static and cyclic creep rate have the same value of 3 as shown in Fig. 1. To interpret the meaning of this stress exponent value for the cyclic creep rate, it may be worthwhile to consider the effect of grain boundary sliding on the total deformation. Davies *et al.* [12] have suggested that the total elongation, ε_t, is given by

$$\varepsilon_t = \varepsilon_g + \varepsilon_{gb}$$

where ε_{gb} is the elongation resulting from grain boundary sliding and ε_g is the mean elongation of the grain. Thus, the apparent creep rate can be expressed as $\dot{\varepsilon}_t = \dot{\varepsilon}_g + \dot{\varepsilon}_{gb}$. In this work, as shown in Fig. 1, the stress exponent $\dot{\varepsilon}_t$ is found to be 3, independent of the stress mode.

In temperature and stress ranges equivalent to those of this work, Oikawa *et al.* [7] report that the stress exponent of static creep is also 3, for which ε_g is more dominant in the creep deformation, and this agrees with our result. But, as shown in Table II, since ε_g varies with the stress mode one must consider the

TABLE II

Property*	Stress mode					
	Static	Cyclic (loading rates = 15 MPa in 2.1 sec) On-load time (sec)				
		18	14	12	10	4
$\bar{W}$	2.112	1.644	1.496	1.415	1.140	1.028
ε_g	0.646	0.393	0.308	0.260	0.091	0.019
ε_t	0.57	0.56	0.42	0.40	0.40	0.17
Creep rate ($\times 10^{-6}$ sec^{-1})	1.90	2.00	1.81	1.15	0.99	0.42
Rupture strain	> 60%	> 60%	> 60%	39.8%	39.6%	11.3%

*$\bar{W} = \bar{b}/\bar{a}$ where $\bar{a}$ = average elongation of each grain perpendicular to the stress axis and $\bar{b}$ = average elongation parallel to the stress axis; $\varepsilon_g = (\bar{W})^{2/3} - 1$.

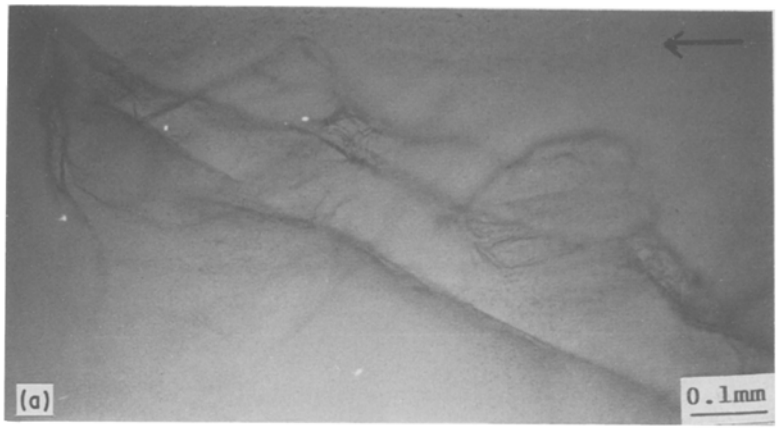

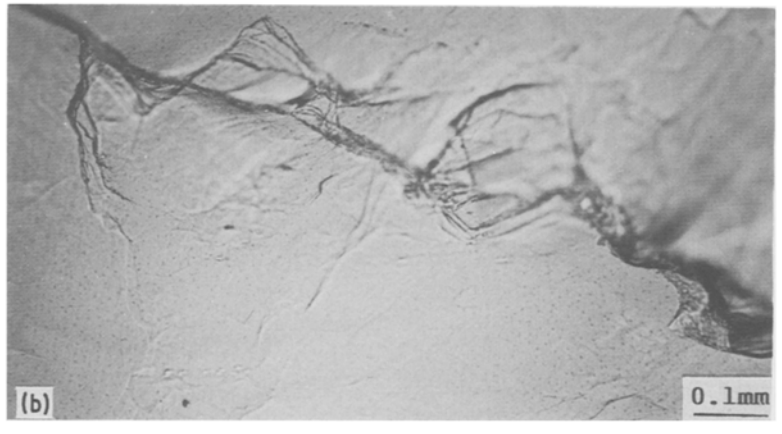

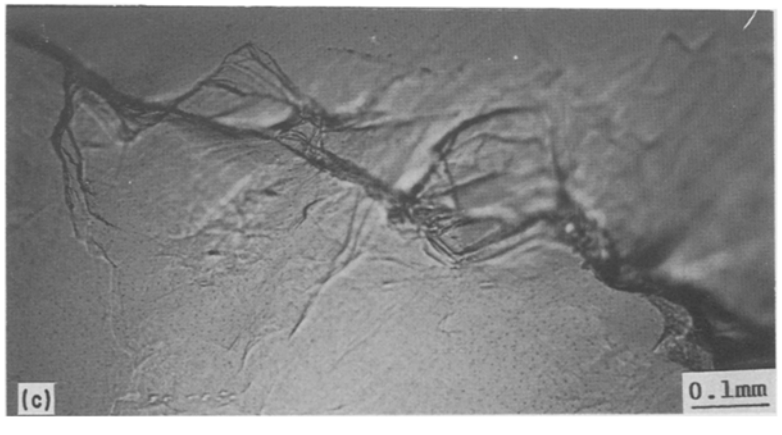

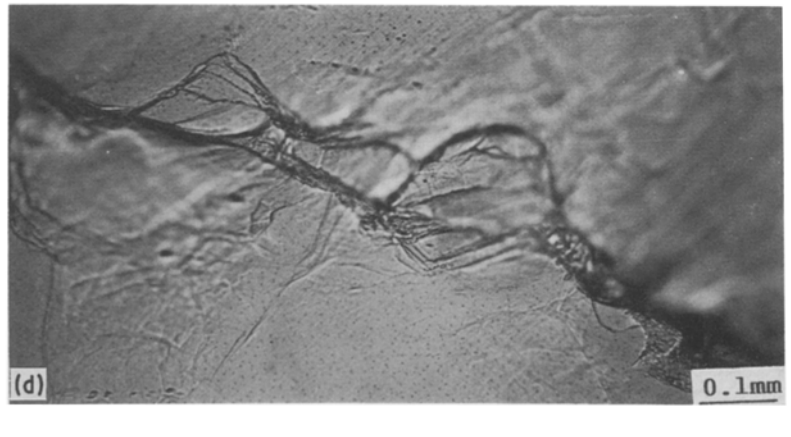

Figure 7 Metallographic observation of statically crept specimens; stress 15 MPa. (a) 5% creep strain, (b) 10% creep strain, (c) 15% creep strain, (d) 20% creep strain.

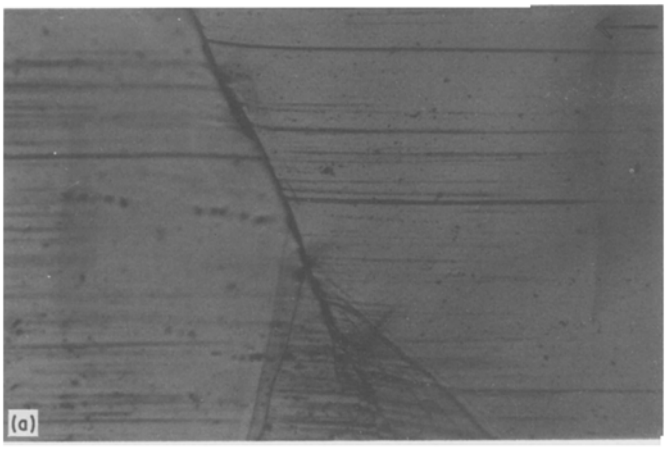

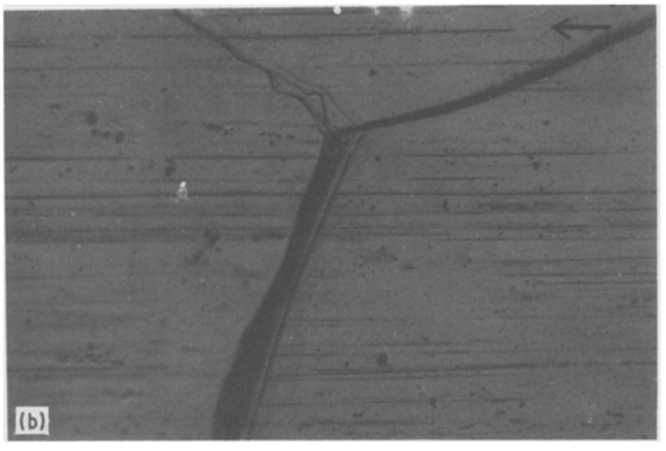

Figure 8 (a, b) Metallographic observation of cyclically crept specimens. Cyclic stress conditions 15 MPa, 3 cycles per minute, stress amplitude 90%, amount of creep strain 10%.

effect of ε_{gb} on the total deformation. Horton [13] reported that the stress exponent of the grain boundary sliding rate, $\dot{\varepsilon}_{gb}$, was about 3, which was independent of the solute contents. On the basis of the above-mentioned reports, one may deduce that even if the fraction of ε_{gb} in ε_t varies, the stress exponent of the creep rate should not be changed.

Evaluating the results for the value of stress exponent, substructure and transient phenomena, Oikawa *et al.* [7] and Yavari and Longdon [6] have reported that dislocation glide was a dominant creep deformation process in Al–Mg alloys. Considering the stress exponent obtained in this investigation, we can also say that dislocation glide is one of the deformation processes in the deformation of a grain over the stress and temperature ranges in this work.

4.3. Cyclic stress effects on the grain boundary deformation

As the deformation proceeds, it is observed that the grain boundaries are sharply serrated in the statically crept specimens (Fig. 7); however, in the cyclically crept specimens in which grain boundary sliding still appears the boundaries remain straight (Fig. 4c). If the sliding process depends upon the mechanism of alternately occurring dislocation glide and climb

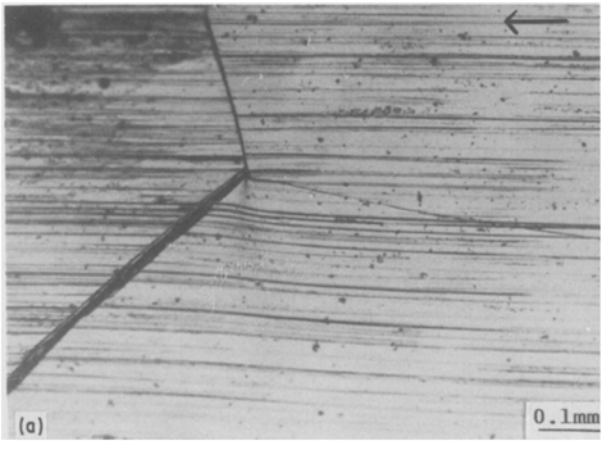

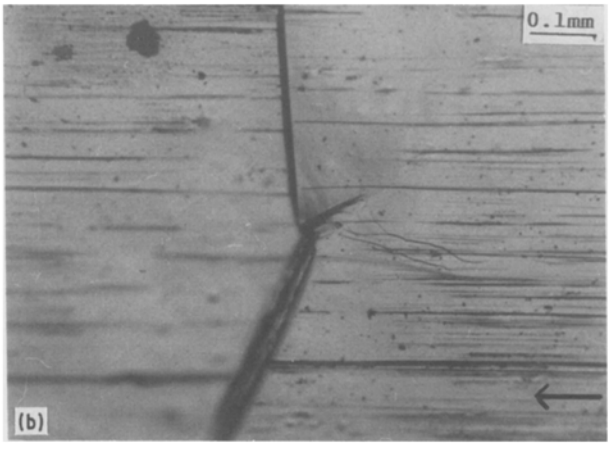

Figure 9 Fold formation at (a) a triple point, (b) a curved grain boundary. Cyclic stress conditions = 15 MPa, 3 cycles per minute, stress amplitude = 90%.

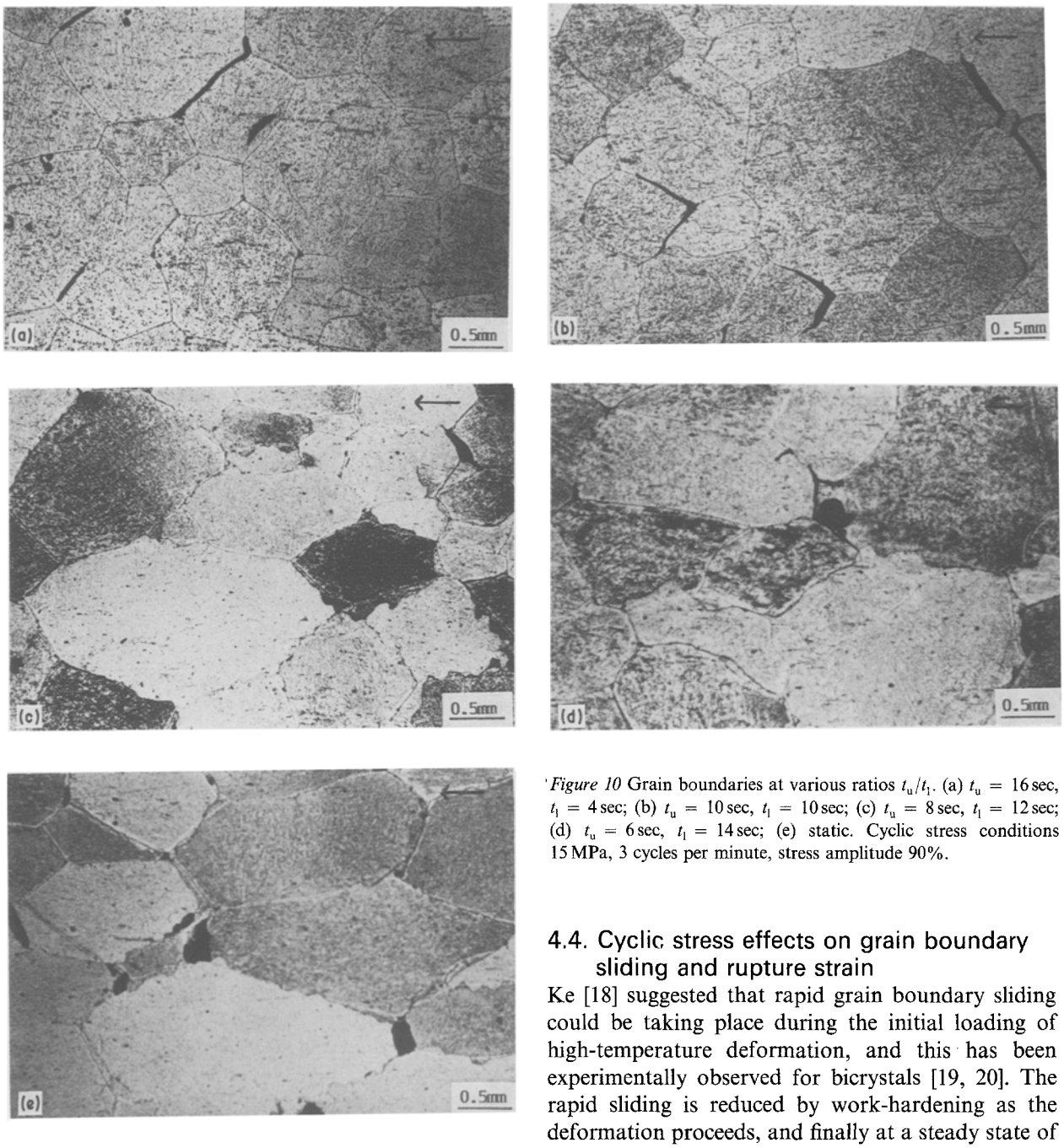

Figure 10 Grain boundaries at various ratios t_u/t_l. (a) $t_u = 16$ sec, $t_l = 4$ sec; (b) $t_u = 10$ sec, $t_l = 10$ sec; (c) $t_u = 8$ sec, $t_l = 12$ sec; (d) $t_u = 6$ sec, $t_l = 14$ sec; (e) static. Cyclic stress conditions 15 MPa, 3 cycles per minute, stress amplitude 90%.

along the grain boundary, the sliding is inhibited more at an irregular grain boundary than that at a smooth grain boundary, because irregular deformation is due to the substructure near the grain boundary [14].

It has been suggested by many authors that the cyclic creep rate can be accelerated by a recovery process assisted either by plastically generated excess point defects [15, 16] or cross-slip of screw dislocations [17]. If the substructure is formed near the grain boundary as suggested by Lytton *et al.* [14], the recovery in this region can be accelerated by cyclic stress, which results in a less irregular grain boundary. So, in cyclic creep, the grain boundary is less serrated by irregular boundary migration and sliding can easily occur at this less serrated grain boundary. One can see also in Fig. 4 that the region of migration is narrow and the sliding occurred at this smooth grain boundary.

4.4. Cyclic stress effects on grain boundary sliding and rupture strain

Ke [18] suggested that rapid grain boundary sliding could be taking place during the initial loading of high-temperature deformation, and this has been experimentally observed for bicrystals [19, 20]. The rapid sliding is reduced by work-hardening as the deformation proceeds, and finally at a steady state of static creep the sliding rate becomes very slow. A sliding hardening mechanism has been suggested by many authors [1, 12, 13, 19, 21, 22] in terms of the interaction between deformation at the grain boundary and in the grain. There has been no report on the fraction of boundary sliding in migration for the duration of on-load time during cyclic creep, but there are some experimental reports which explain that the fraction of sliding in the total deformation is larger during the primary stage of static creep and decreases as the deformation proceeds [12, 20]. On the basis of these experimental reports and our observations in which every on-load period of the steady state in cyclic creep is known to be equivalent to the primary state of static creep, boundary sliding may be taking place during the period of on-load time in cyclic creep deformation. As shown schematically in Fig. 6 for the first few seconds of the on-load period, cyclic creep deformation rate is very fast (same trend as the primary stage in static creep); however, as the on-load time passes the rate becomes very slow. Thus, one may guess that, if

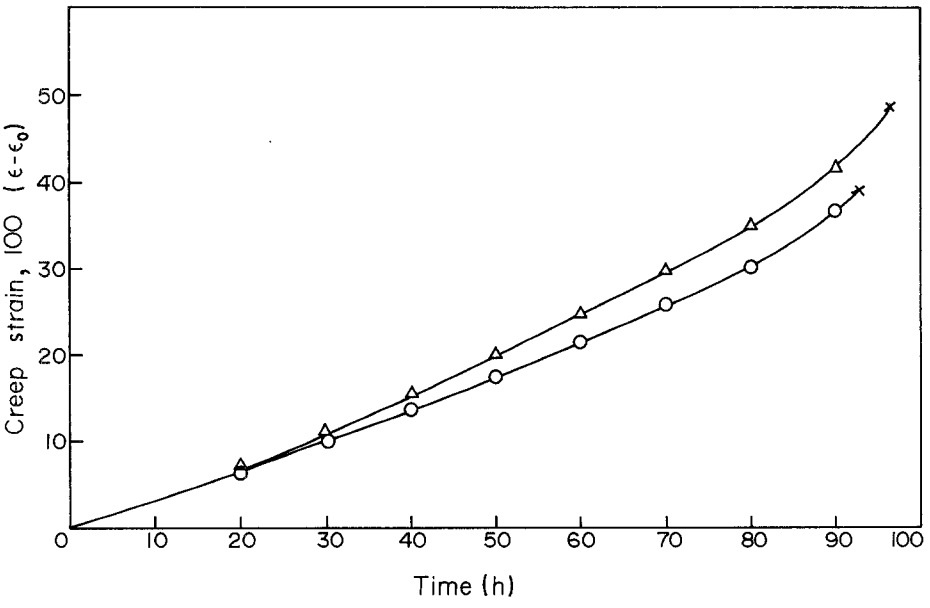

Figure 11 Cyclic creep curves at 580 K for (△) slow loading (15 MPa in 2 sec) and (○) fast loading (15 MPa in 0.3 sec). Frequency 3 cycles per minute, $\Delta\sigma/\sigma = 0.9$, stress 15 MPa.

the duration of the on-load time is decreased to exclude the portion of time during which the rate is very slow, the sliding fraction will be larger and the rupture strain will also be decreased. Table II gives the experimental results which show that the rupture strain is reduced and the fraction of sliding is increased as the ratio t_l/t_u decreases, while the stress frequency and amplitude are kept constant.

When the frequency of the cyclic stress changes from 3 to 1 cycle per minute or the stress amplitude changes from 90 to 10% of the peak stress, the specimen does not rupture even after it has been crept more than 60% of creep strain. When the frequency of the cyclic stress was 1 cycle per minute, the elongation per period was larger than that of 3 cycles per minute by about 3 times, which results in more slide hardening per period by this large deformation. At a stress amplitude of 10%, the driving force for the recovery during the off-load time is too small for the recovery to take place.

The loading rate of cyclic creep may have an influence on crack formation at a triple point which acts as a stress accumulating point. By using the finite element method (FEM), Riedel [23] suggests that if there exists a stress concentration spot, such as a crack tip, depending on the loading rate the stress concentration in dynamic loading may become larger than that in static loading. From Riedel's calculations, it is shown that the amount of stress concentration is smaller with a slower loading rate. This implies that if a slower loading rate is applied the crack formation and propagation will be retarded so that the rupture strain may be increased. As shown in Fig. 11, the cyclic creep rupture strain with a slower loading rate (15 MPa in 2.1 sec) is larger than that with the faster rate (15 MPa in 0.3 sec).

In this experimental range, where grain boundary cracks can be observed during cyclic creep, the dislocation structure in a grain is shown in Fig. 12a (statically crept specimen) and Fig. 12b (cyclically crept specimen). As shown at Fig. 12, the dislocations are distributed homogeneously and the difference between the dislocation structure of a statically crept specimen and that of a cyclically crept specimen cannot be observed. Fig. 13 shows the dislocation structure near the grain boundary. Ledges of fine scale can be

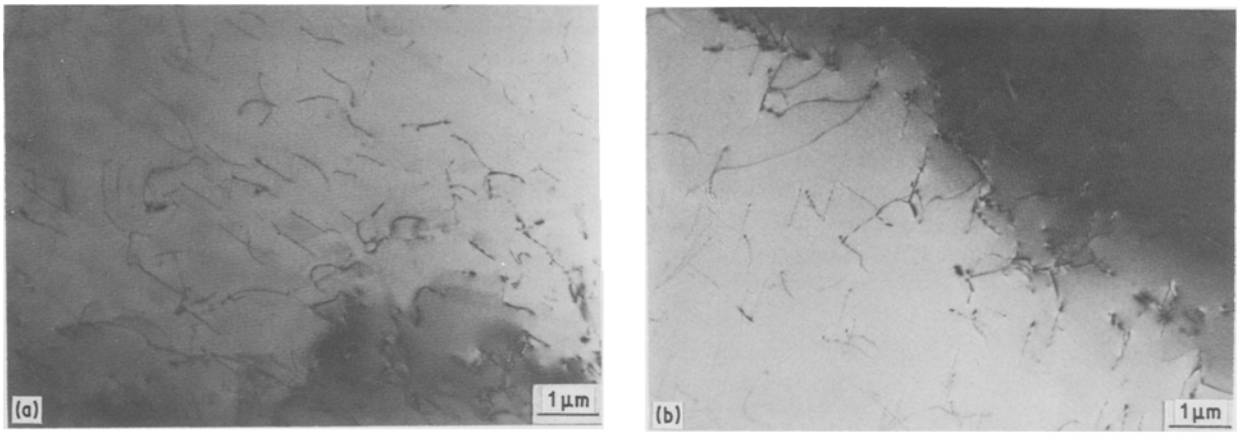

Figure 12 Dislocation configurations in grains. (a) Statically crept specimen, creep strain 20%; (b) cyclically crept specimen, creep strain 20%.

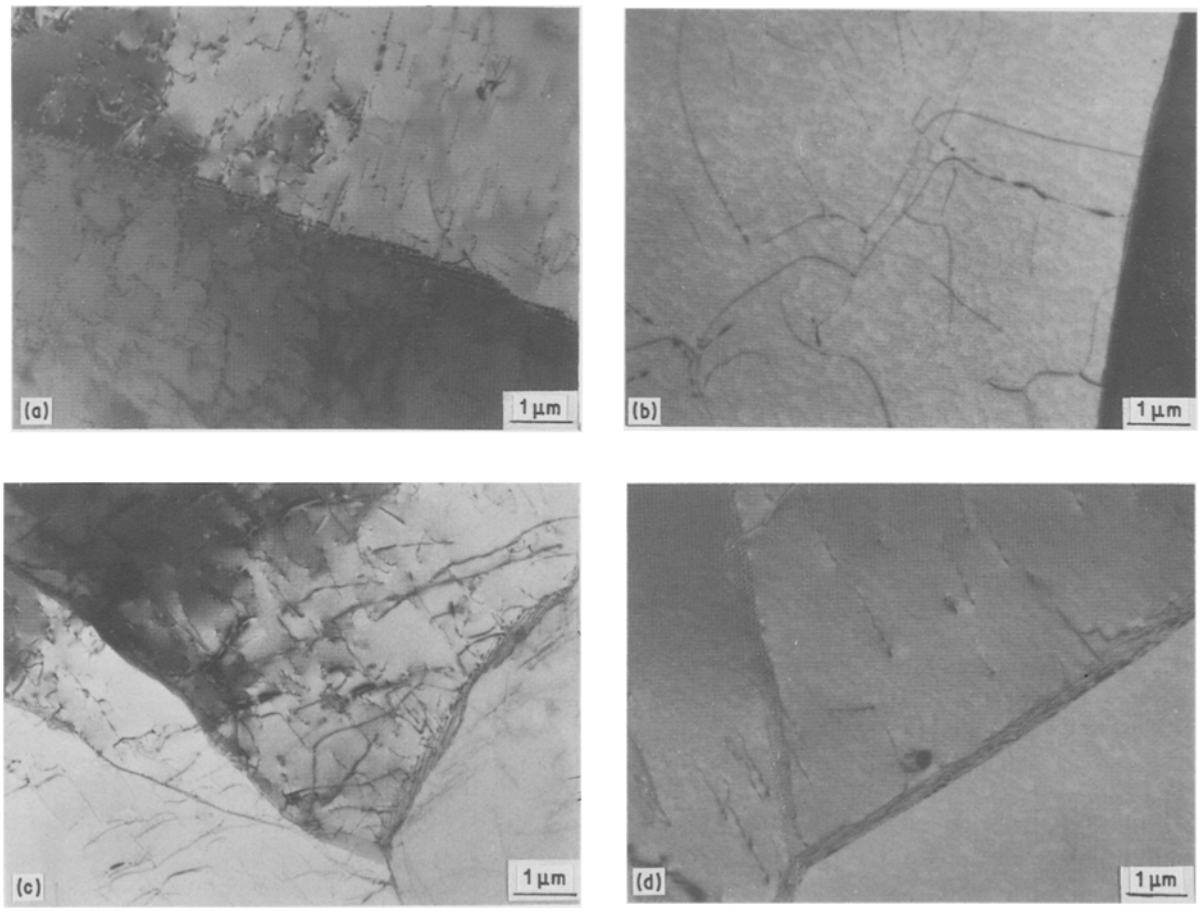

Figure 13 Dislocation configurations near the grain boundary. (a, c) Statically crept specimen, creep strain 20%, creep stress 15 MPa; (b, d) cyclically crept specimen, creep strain 20%, cyclic stress conditions = 15 MPa, 3 cycles per minute, stress amplitude = 90%.

observed at the grain boundaries of the statically crept specimen but we cannot observe these in the case of cyclic creep. Fig. 13c shows the triple point of a statically crept specimen, where the grain boundaries are severely curved and migrated, and the dislocations are more tangled. However, for the case of the cyclically crept specimen, the grain boundaries at the triple point are straight and not deformed, as shown in Fig. 13d.

From these observations, it can be said that cyclic stress only affected the grain boundary deformation and enhanced the recovery near the grain boundaries.

5. Conclusions

The following conclusions are drawn from the experimental data:

1. The fraction of grain boundary sliding in the total creep deformation is larger, and the rupture strain smaller, for cyclic creep compared with static creep.

2. With the same amount of creep strain, for statically crept specimens the grain boundaries are severely serrated by boundary migration, while the grain boundaries remain straight after sliding for the cyclically crept specimens.

3. As the fraction of off-load time increases while the stress frequency and amplitude are kept constant, the extent of recovery near a grain boundary increases.

4. The recovery near a grain boundary is believed to be enhanced by cyclic stress due to the excess vacancies athermally generated. The recovery near a grain boundary can make the boundary less serrated and so the sliding becomes easier. So, the fraction of sliding is increased and the rupture strain decreases because the crack at a triple point is formed by the stress accumulation due to grain boundary sliding.

References

1. H. BRUNNER and N. J. GRANT, *Trans. AIME* **215** (1959) 48.
2. H. C. CHANG and N. J. GRANT, *J. Metals* (May 1956) **8**, *Trans. AIME* **206** (1956) 544.
3. *Idem, ibid.* (February, 1953) 305.
4. I. S. CHOI and S. W. NAM, Korea Patent No. 85-1260 (1985).
5. C. J. SMITHELLS, "Metals Reference Book", Vol. 1 (Butterworths, London, 1978) p. 301.
6. P. YAVARI and T. G. LANGDON, *Acta Metall.* **30** (1982) 2181.
7. H. OIGAWA, K. SUGAWARA and S. KARASHIMA, *Scripta Metall.* **10** (1976) 885.
8. W. A. RACHINGER, *J. Inst. Metals* **81** (1952–53) 33.
9. K. W. SNOWDEN, *Phil. Mag.* **14** (1966) 1019.
10. A. H. COTTRELL, "Structural Processes in Creep" (Iron and Steel Institute, London, 1961) p. 1.
11. A. N. STROTH, *Proc. R. Soc.* **A218** (1953) 391.
12. P. W. DAVIES, R. N. STEVENS and B. WILSHIRE, *J. Inst. Metals* **94** (1966) 49.
13. C. A. P. HORTON, *Acta. Metall.* **18** (1970) 1159.
14. J. L. LYTTON, C. R. BARRETT and O. D. SHERBY, *Trans. AIME* **233** (1965) 1399.
15. A. J. KENNEDY, in Proceedings of International Conference on Fatigue Metals, 1956, London, p. 401.
16. D. H. SHIN, I. S. CHOI and S. W. NAM, *J. Mater. Sci. Lett.* **2** (1983) 688.

17. P. S. G. BENNETT and J. T. EVANS, *Met. Sci. Eng.* **38** (1979) 111.
18. T. S. KE, *Phys. Rev.* **71** (1947) 533.
19. J. L. WALTER and H. E. CLINE, *Trans. AIME* **242** (1968) 1823.
20. T. WATANABE and P. W. DAVIES, *Phil. Mag.* **A37** (1978) 649.
21. T. WATANABE, M. YAMADA, S. SHIMA and S. KARASHIMA, *ibid.* **A40** (1979) 667.
22. K. E. PUTTICK and B. TUCK, *Acta Metall.* **13** (1965) 1043.
23. H. RIEDEL, "Elastic-Plastic Fracture", ASTM STP 83, edited by C. F. Shih and J. P. Gudas (American Society for Testing and Materials, Philadelphia, Pennsylvania, 1981) p. I-505.

Received 23 September 1985
and accepted 18 June 1987